Geomechanics and Engineering, *Vol. 37, No. 3 (2024) 243-251*
https://doi.org/10.12989/gae.2024.37.3.243

The effect of magnetic field and inclined load on a poro-thermoelastic medium using the three-phase-lag model

Samia M. Said*

Department of Mathematics, Faculty of Science, Zagazig University, P.O. Box 44519, Zagazig, Egypt

(*Received February 20, 2024, Revised April 3, 2024, Accepted April 15, 2024*)

Abstract. In the current work, a poro-thermoelastic half-space issue with temperature-dependent characteristics and an inclined load is examined in the framework of the three-phase-lag model (3PHL) while taking into account the effects of magnetic and gravity fields. The resulting coupled governing equations are non-dimensional and are solved by normal mode analysis. To investigate the impacts of the gravitational field, magnetic field, inclined load, and an empirical material constant, numerical findings are graphically displayed. MATLAB software is used for numerical calculations. Graphs are used to visualize and analyze the computational findings. It is found that the physical quantities are affected by the magnetic field, gravity field, the nonlocal parameter, the inclined load, and the empirical material constant.

Keywords: gravity field; inclined load; magnetic field; normal mode analysis; porous material; properties; temperature-dependent; three-phase-lag model

1. Introduction

The simplest generalization of the classical theory of elasticity is the idea of elastic solids with voids. It is important to keep in mind that porous materials have applications in many engineering fields, including the petroleum industry, material science, and biology. This theory focuses on elastic materials made up of a distribution of small porous (voids), in which the void volume is included among the kinematic variables. Cowin and Nunziato (1973) talked about elastic materials with vacancies and their linear theory. Nunziato and Cowin (1979) conducted the first study in the theory of thermoelastic materials with voids. Iesan (1986) established the uniqueness, reciprocity, and variational theorems as well as developed the theory of thermoelastic material with voids. The nonlinear theory of non-simple thermoelastic materials with vacancies was covered by Ciarletta and Scalia (1993). The sphere of impact and uniqueness that lead to thermoelastic solids with voids were examined by Marin (1996, 1997). The deformation resulting from moving loads in a thermoelastic media with voids was first described by Kumar and Rani (2006). Quintanilla (2009) demonstrated the validity of uniqueness theorems in the dynamic theory of porous media thermoelasticity at microtemperatures. Numerous issues pertaining to wave propagation in a thermoelastic porous medium were examined by Marin *et al*. (2015), Othman *et al.* (2020), Hobiny and Abbas (2020), Biswas (2021), Tantawy and Zenkour (2023), Fahmy *et al*. (2011, 2018, 2019a, b, c, 2021a, b, 2023), Marin *et al*. (2022), Said *et al*. (2022, 2024).

Research on wave propagation in generalized thermoelasticity materials has potential applications in seismology, geophysics, and structural engineering. If gravity is taken into consideration, this kind of investigation becomes more feasible. The effects of gravity on wave propagation in solids, particularly on elastic spheres, were originally studied by Bromwich (1898). However, Biot (1965) discusses the impact of the elastic surface waves' gravity field. The axisymmetric problem of wave propagation under gravity in a medium consisting of a liquid layer and an underlying solid half-space was investigated by Nath and Sengupta (1999). Ahmed (2005) studied the effects of a gravity field on Stoneley waves in a non-homogeneous isotropic granular material. The impact of the gravity field on an orthotropic elastic media for various theories was examined by Abd-Alla *et al*. (2011). Under the impact of gravity, Othman *et al*. (2013) developed the generalized thermoelastic medium with temperature-dependent features for three theories. Studies on the impact of gravity field on various thermoelastic media have been published by Jain *et al*. (2018), Zenkour (2020), Alharbi *et al.* (2021), Abbas *et al.* (2015, 2020, 2019, 2021a, b), and Said (2023, 2024).

Thermoelasticity theories, which describe heat flow and deformation in a continuum, have received a lot of attention in recent years. A material body transmits mechanical waves when it is loaded or subjected to an external force. For instance, thermal expansion causes a solid body to suddenly heat up, producing a mechanical wave. One of continuum dynamics' most comprehensive and fruitful fields of study is the interplay between mechanical and thermal fields. Since most structural components of heavy industries are often associated with mechanical and thermal stresses at elevated temperatures, the suggested model is useful in determining the kind of interaction between

*Corresponding author, Professor
E-mail: samia_said59@yahoo.com

ISSN: 2005-307X (Print), 2092-6219 (Online)

mechanical and thermal forces. Studies on the impact of inclined load on various thermoelastic mediums have been published by Kumar and Aliwalia (2007), Othman *et al.* (2009), Sharma *et al*. (2015), Abouelregal and Zenkour (2016), Lata *et al.* (2019a, b, 2022), Deswal *et al*. (2020), Alharbi (2021), and De *et al*. (2023).

In the current work, the three-phase lag model has been used to tackle the two-dimensional deformation problem of a magneto-thermoelastic porous material with temperature-dependent characteristics and inclined load. The analytical solution of physical fields is seen using the normal mode analysis. Comparative analysis was done between the variables under consideration for various values of gravity field, magnetic field, inclined load, and empirical material constant values. Graphs are used to visualize and analyze the computational findings. It is found that the physical quantities are affected by the magnetic field, gravity field, the nonlocal parameter, the inclined load, and the empirical material constant.

2. Formulation of the problem

We consider an isotropic, homogeneous, thermally conducting thermoelastic porous material half-space ($x\geq 0$). The displacement components have the form $\boldsymbol{u} = (u, o, w)$. The medium permeated into a uniform magnetic field with a constant intensity $\boldsymbol{H}(0,H_0,0)$ under the effect of gravity field. The fundamental equations of the generalized thermoelasticity are:

According to Alharbi *et al.* (2021) and Hetnarski and Eslami (2009), the stress-strain relations.

$$\sigma_{ij} = 2\,\mu e_{ij} + (\lambda e + b\varphi - \gamma \hat{T})\delta_{ij}\,. \tag{1}$$

Equation of motion

$$\rho u_{i,tt} = \sigma_{ij,j} + \mu_0 (\boldsymbol{J}\times\boldsymbol{H})_i + F_i\,, \tag{2}$$

$$\beta\varphi_{,ii} - be - \alpha_1\varphi - \alpha_2\varphi_{,t} + \alpha_3\hat{T} = \rho\,\alpha_4\,\varphi_{,tt}\,. \tag{3}$$

Where $F_1 = \rho g\dfrac{\partial w}{\partial x}, F_2 = 0, F_3 = \rho g\dfrac{\partial u}{\partial x}$ are force due to the presence of the gravity field.

The heat equation as Choudhuri (2007)

$$\left(1+\tau_q\frac{\partial}{\partial t}+\frac{1}{2}\tau_q^2\frac{\partial^2}{\partial t^2}\right)(\rho C_E T_{,tt} + \gamma T_0 e_{,tt} + \alpha_3 T_0\varphi_{,tt}) = K\left(1+\tau_T\frac{\partial}{\partial t}\right)T_{,tii} + K^*\left(1+\tau_v\frac{\partial}{\partial t}\right)T_{,ii}\,. \tag{4}$$

We assume that as Othman *et al.* (2013)

$$\mu = \mu_1(1-\theta_0 T_0),\quad \lambda = \lambda_1(1-\theta_0 T_0),\quad \gamma = \gamma_1(1-\theta_0 T_0),$$
$$b = b_1(1-\theta_0 T_0),\quad \alpha_1 = \alpha_{11}(1-\theta_0 T_0),\quad \alpha_2 = \alpha_{21}(1-\theta_0 T_0), \tag{5}$$
$$\alpha_3 = \alpha_{31}(1-\theta_0 T_0),\quad \alpha_4 = \alpha_{41}(1-\theta_0 T_0).$$

In the case of the temperature-independent modulus of elasticity $\theta_0 = 0$.

Introducing Eqs. (1) in Eq. (2), we get

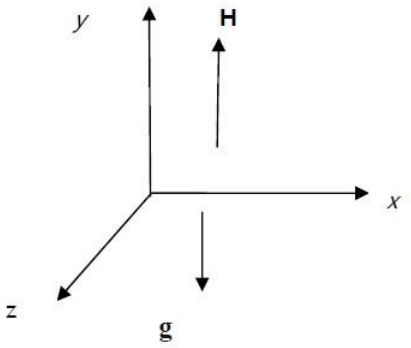

Fig. 1 Geometry of the problem

$$\left(\rho+\varepsilon_0\mu_0^2H_0^2\right)\frac{\partial^2 u}{\partial t^2} = (\lambda+2\mu)\frac{\partial^2 u}{\partial x^2} + (\lambda+\mu)\frac{\partial^2 w}{\partial x\partial z} + \mu\frac{\partial^2 u}{\partial z^2} + b\frac{\partial\varphi}{\partial x} - \gamma\frac{\partial\hat{T}}{\partial x} + \rho g\frac{\partial w}{\partial x} - \mu_0 H_0\frac{\partial h}{\partial x}, \tag{6}$$

$$\left(\rho+\varepsilon_0\mu_0^2H_0^2\right)\frac{\partial^2 w}{\partial t^2} = (\lambda+2\mu)\frac{\partial^2 w}{\partial z^2} + (\lambda+\mu)\frac{\partial^2 u}{\partial x\partial z} + \mu\frac{\partial^2 w}{\partial x^2} + b\frac{\partial\varphi}{\partial z} - \gamma\frac{\partial\hat{T}}{\partial z} - \rho g\frac{\partial u}{\partial x} - \mu_0 H_0\frac{\partial h}{\partial z}. \tag{7}$$

Introducing the following non-dimension quantities

$$(x',z',u',w') = c_1\eta(x,z,u,w),\ g' = \frac{g}{\eta c_1^3},\ \theta = \frac{\gamma\hat{T}}{(\lambda+2\mu)},\ \varphi' = \varphi,$$
$$(t',\tau_q',\tau_v',\tau_T') = c_1^2\eta(t,\tau_q,\tau_v,\tau_T),\ \sigma_{ij}' = \frac{\sigma_{ij}}{\mu},\qquad h' = \frac{h}{H_0}, \tag{8}$$

where $\eta = \dfrac{\rho C_E}{K^*}$, $\qquad c_1^2 = \dfrac{(\lambda+2\mu)}{\rho}$.

The governing equations reduce to in terms of the non-dimensional quantities described above (dropping the dashed for convenience)

$$\pi\frac{\partial^2 u}{\partial t^2} = \frac{\partial^2 u}{\partial x^2} + \pi_2\frac{\partial^2 w}{\partial x\partial z} + \pi_1\frac{\partial^2 u}{\partial z^2} + \pi_3\frac{\partial\varphi}{\partial x} - \frac{\partial\theta}{\partial x} + g\frac{\partial w}{\partial x} - \pi_4\frac{\partial h}{\partial x}, \tag{9}$$

$$\pi\frac{\partial^2 w}{\partial t^2} = \pi_1\frac{\partial^2 w}{\partial x^2} + \pi_2\frac{\partial^2 u}{\partial x\partial z} + \frac{\partial^2 w}{\partial z^2} + \pi_3\frac{\partial\varphi}{\partial z} - \frac{\partial\theta}{\partial z} - g\frac{\partial u}{\partial x} - \pi_4\frac{\partial h}{\partial z}, \tag{10}$$

$$\varphi_{,ii} - \varpi_1 e - \varpi_2\varphi - \varpi_3\frac{\partial\varphi}{\partial t} + \varpi_4\theta = \varpi_5\frac{\partial^2\varphi}{\partial t^2}, \tag{11}$$

$$\left(1+\tau_q\frac{\partial}{\partial t}+\frac{1}{2}\tau_q^2\frac{\partial^2}{\partial t^2}\right)(\theta_{,tt} + \pi_7 e_{,tt} + \pi_0\varphi_{,tt}) = \pi_8\left(1+\tau_T\frac{\partial}{\partial t}\right)\theta_{,tii} + \pi_9\left(1+\tau_v\frac{\partial}{\partial t}\right)\theta_{,ii}. \tag{12}$$

3. Normal mode analysis

The solution of the considered physical variable can be decomposed in terms of normal modes in the form

$$[u,w,\theta,\varphi,\sigma_{ij}](x,z,t) = [u^*,w^*,\theta^*,\varphi^*,\sigma_{ij}^*](z)\exp(mt+\mathrm{i}Bx), \tag{13}$$

where $u^*(z), w^*(z), \varphi^*(z), \theta^*(z), \sigma_{ij}^*(z)$ are the amplitudes of the field quantities.

Using Eq. (13), Eqs. (9)-(12) become respectively

$$\left(\pi_1 \mathrm{D}^2 - \pi_{10}\right) u^* + \mathrm{i}B\left(\pi_6 \mathrm{D} + \mathrm{g}\right) w^* + \mathrm{i}B\pi_3 \varphi^* = \mathrm{i}B\theta^*, \quad (14)$$

$$\mathrm{i}B\left(\pi_6 \mathrm{D} - \mathrm{g}\right) u^* + \left(\pi_5 \mathrm{D}^2 - \pi_{11}\right) w^* + \pi_3 \mathrm{D}\varphi^* = \mathrm{D}\theta^*, \quad (15)$$

$$\mathrm{i}B\varpi_1 u^* + \varpi_1 \mathrm{D} w^* - \left(\mathrm{D}^2 - \pi_{12}\right)\varphi^* = \varpi_4 \theta^*, \quad (16)$$

$$\mathrm{i}m_1\pi_7 \mathrm{B}u^* + m_1\pi_7 \mathrm{D}w^* + m_1\pi_0 \varphi^* = \left(\pi_{13}\mathrm{D}^2 - \pi_{14}\right)\theta^*. \quad (17)$$

Eliminating $w^*(z)$, $\theta^*(z)$ and $\varphi^*(z)$ between Eqs. (14)-(17), we obtain the eighth-order ordinary differential equation satisfied with $u^*(z)$,

$$[\mathrm{D}^8 - \chi_1 \mathrm{D}^6 + \chi_2 \mathrm{D}^4 - \chi_3 \mathrm{D}^2 + \chi_4] u^*(z) = 0, \quad (18)$$

where $\pi, \pi_i, i = 1, 2, 3, ..., 26$, ϖ_j, $i = 1, 2, 3, ..., 6$, χ_n, $n = 1, 2, 3, 4$ are given in **Appendix.**

In a physical problem, we suppress the positive exponentials unlimited at infinity. So the solution of Eq. (18), which is bound as $z \to \infty$, is given by

$$u^*(z) = \sum_{n=1}^{4} \Gamma_n \exp(-R_n z), \quad (19)$$

$$w^*(z) = \sum_{n=1}^{4} \Delta_{1n} \Gamma_n \exp(-R_n z), \quad (20)$$

$$\theta^*(x) = \sum_{n=1}^{4} \Delta_{2n} \Gamma_n \exp(-R_n z), \quad (21)$$

$$\varphi^*(x) = \sum_{n=1}^{4} \Delta_{3n} \Gamma_n \exp(-R_n z), \quad (22)$$

where $R_n^2 (n = 1, 2, 3, 4)$ are the roots of the characteristic equation of Eq. (18), and $\Delta_{\mathrm{in}} (i = 1, 2, 3)$ are given in **Appendix.**

Using Eqs. (8), (13), and (19)-(22) in Eq. (1), thus we have

$$\sigma_{zz}^*(z) = \sum_{n=1}^{4} \Delta_{4n} \Gamma_n \exp(-R_n z), \quad (23)$$

$$\sigma_{xz}^*(z) = \sum_{n=1}^{4} \Delta_{5n} \Gamma_n \exp(-R_n z), \quad (24)$$

where Δ_{4n}, Δ_{5n} are given in **Appendix.**

The normal mode analysis is, in fact, to look for the solution in the Fourier transform domain, assuming that all the field quantities are sufficiently smooth on the real line such that normal mode analysis of these functions exists.

4. Boundary conditions

To determine the unknown parameters $\Gamma_n (n = 1, 2, 3, 4)$ we can take the following boundary conditions:

a) The mechanical boundary condition that an inclined force is applied to the half-space surface as Othman *et al*. (2009)

$$\begin{aligned} \sigma_{zz}(0, x, t) &= -f_0 \cos(\phi) \exp(mt + \mathrm{i}Bx), \\ \sigma_{xz}(0, x, t) &= -f_0 \sin(\phi) \exp(mt + \mathrm{i}Bx). \end{aligned} \quad (25)$$

b) We can interpret the change in the volume fraction field of voids at the free surface as

$$\varphi = 0. \quad (26)$$

c) On the half-space surface, the thermal boundary condition is

$$\theta = 0. \quad (27)$$

where f_0 is a constant. Using the above boundary conditions, we can obtain

$$\begin{aligned} &\sum_{n=1}^{4} \Delta_{2n} \Gamma_n = 0, \qquad \sum_{n=1}^{4} \Delta_{3n} \Gamma_n = 0, \\ &\sum_{n=1}^{4} \Delta_{4n} \Gamma_n = -f_0 \cos(\phi), \qquad \sum_{n=1}^{4} \Delta_{5n} \Gamma_n = -f_0 \sin(\phi). \end{aligned} \quad (28)$$

Solving the above system of Eqs. (28), we obtain a system of four equations. After applying the inverse of the matrix method, we have the values of the four constants $\Gamma_n (n = 1, 2, 3, 4)$:

$$\begin{pmatrix} \Gamma_1 \\ \Gamma_2 \\ \Gamma_3 \\ \Gamma_4 \end{pmatrix} = \begin{pmatrix} \Delta_{21} & \Delta_{22} & \Delta_{23} & \Delta_{24} \\ \Delta_{31} & \Delta_{32} & \Delta_{33} & \Delta_{34} \\ \Delta_{41} & \Delta_{42} & \Delta_{43} & \Delta_{44} \\ \Delta_{51} & \Delta_{52} & \Delta_{53} & \Delta_{54} \end{pmatrix}^{-1} \begin{pmatrix} 0 \\ 0 \\ -f_0 \cos(\phi) \\ -f_0 \sin(\phi) \end{pmatrix}. \quad (29)$$

5. Numerical results and discussion

Following Said *et al*. (2022), magnesium material was chosen for purposes of numerical evaluations. The physical data of the magnesium (in SI unit) at the distance x=0.5 m as

$\lambda_1 = 3.76 \times 10^{10}\ \mathrm{N.m^{-2}}$, $\mu_1 = 5.86 \times 10^{10}\ \mathrm{N.m^{-2}}$, $\varepsilon_0 = 0.3$,

$\alpha_{41} = 1.753 \times 10^{-10}\ \mathrm{N.m^{-2}}$, $\beta = 2 \times 10^{6}\ \mathrm{N.m^{-2}}$, $\xi = -0.5$,

$C_E = 383..3\ \mathrm{J.kg^{-1}.K^{-1}}$, $m_0 = -0.6$, $\rho = 8954\ \mathrm{kg.m^{-3}}$,

$f_0 = 1.5$, $\tau_q = 9 \times 10^{-5}\mathrm{s}$, $\tau_\upsilon = 6 \times 10^{-5}\mathrm{s}$, $\tau_T = 7 \times 10^{-5}\mathrm{s}$,

$K^* = 386\ \mathrm{w.m^{-1}.K^{-1}}$, $\alpha_{11} = 1.475 \times 10^{10}\ \mathrm{N.m^{-2}}$, $\alpha_{21} = 7.87 \times 10^{-12}\ \mathrm{N.m^{-2}}$,

$T_0 = 298\mathrm{K}$, $\mu_0 = 1.7$, $B = 0.4$, $\alpha_{31} = 2 \times 10^{12}\ \mathrm{N.m^{-2}}$,

$b_1 = 1.6 \times 10^{10}\ \mathrm{N.m^{-2}}$. $\alpha_t = 1.78 \times 10^{-3}\ \mathrm{K^{-1}}$, $K = 386\ \mathrm{w.m^{-1}.K^{-1}.s^{-1}}$,

Figs. 2-4 represent the thermodynamic temperature distribution (Kelvin) θ, the change in volume fraction field distribution φ, and the stress components distributions ($\mathrm{N.m^{-2}}$) σ_{zz} respectively at a constant time against the vertical distance for different values of the magnetic field.

Fig. 2 explains that variation of the thermodynamics temperature (θ) measures in Kelvin begins from a zero value that obeys the boundary conditions. Values of θ decreas reach their minimum value (in amplitude) in the

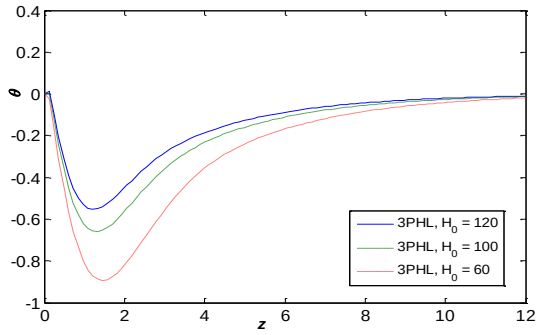

Fig. 2 Thermodynamics temperature θ at varying magnetic field values

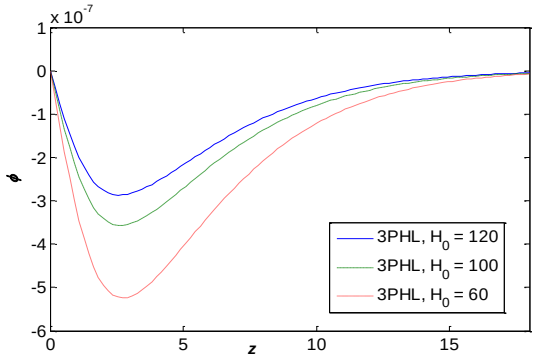

Fig. 3 The change in volume fraction field φ at varying magnetic field values

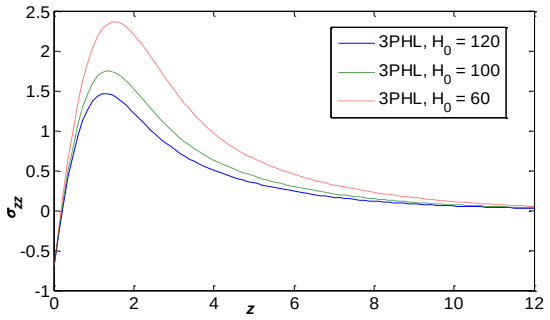

Fig. 4 Distribution of stress component σ_{zz} at varying magnetic field values

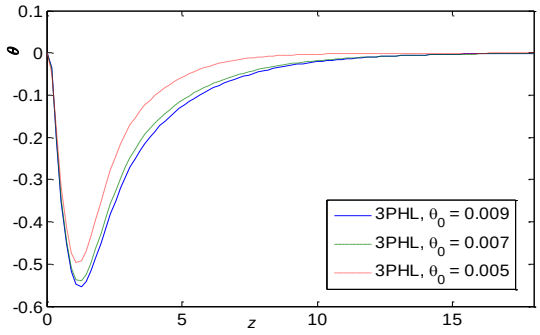

Fig. 5 Thermodynamics temperature θ for varying values of an empirical material constant

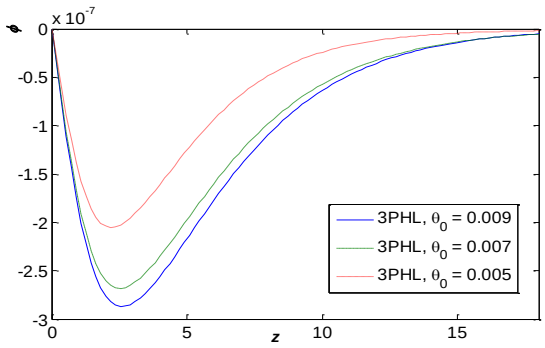

Fig. 6 The change in volume fraction field φ for varying values of an empirical material constant

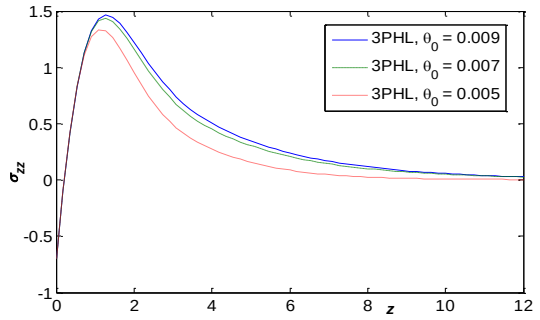

Fig. 7 Distribution of stress component σ_{zz} for varying values of an empirical material constant

range of $0 \le z \le 1.8$, then increase and oscillate like a wave. The magnetic field increases values of θ. Fig. 3 depicts that the variation of change in the volume fraction field φ start from a zero value verified by the boundary condition. Values of φ decrease reach their minimum value (in amplitude) in the range of $0 \le z \le 1.5$, then increases and oscillate like a wave. The magnetic field increases values of φ. Fig. 4 shows that the variation of the stress component σ_{zz} (N.m^{-2}) begins from a negative value and obeys the boundary condition. Values of σ_{zz} increase reach their maximum value (in amplitude) in the range of $0 \le z \le 1.5$, then decrease, and oscillate as a wave. The magnetic field decreases values of σ_{zz}. All the curves begin to coincide when the distance z increases to reach zero at infinity.

Figs. 5-7 represent the thermodynamic temperature distribution (Kelvin) θ, the change in volume fraction field distribution φ, and the stress components distributions (N.m^{-2}) σ_{zz} respectively against the vertical distance for different values of an empirical material constant. Fig. 5 explains that variation of the thermodynamics temperature (θ) measures in Kelvin begins from a zero value that obeys the boundary conditions. Values of θ decrease reach their minimum value (in amplitude) in the range of $0 \le z \le 1.8$, then increase and oscillate like a wave. The empirical material constant decreases values of θ. Fig. 6 depicts that the variation of change in the volume fraction

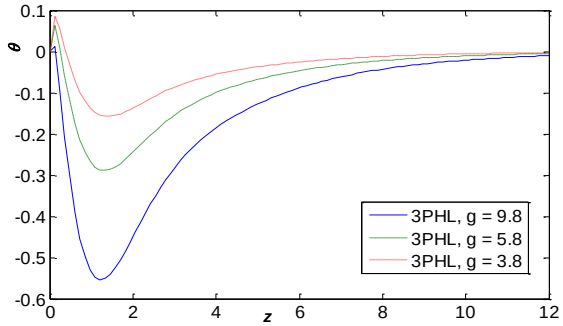

Fig. 8 Thermodynamics temperature θ at varying gravity field values

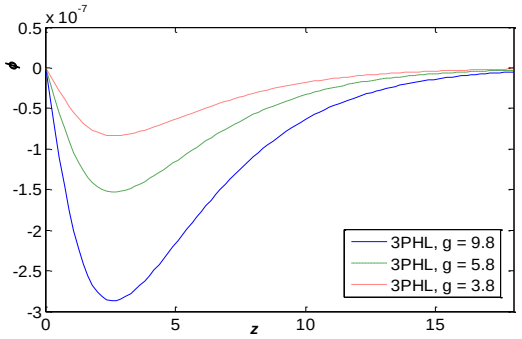

Fig. 9 The change in volume fraction field φ at varying gravity field values

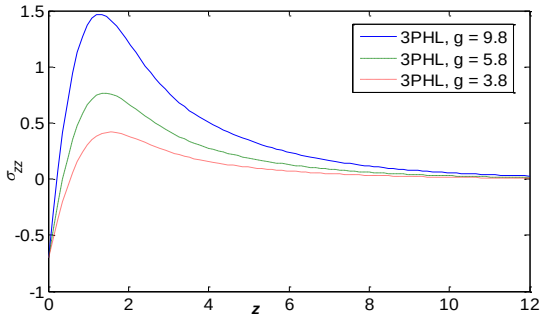

Fig. 10 Distribution of stress component σ_{zz} at varying gravity field values

field φ start from a zero value verified by the boundary condition. Values of φ decrease reach their minimum value (in amplitude) in the range of $0 \le z \le 1.5$, then increase and oscillate like a wave. The empirical material constant decreases values of φ. Fig. 7 shows that the variation of the stress component σ_{zz} (N.m^{-2}) begins from a negative value and obeys the boundary condition. Values of σ_{zz} increase reach their maximum value (in amplitude) in the range of $0 \le z \le 1.5$, then decrease, and oscillate as a wave. The empirical material constant increases values of σ_{zz}.

Figs. 8-10 represent the thermodynamic temperature distribution (Kelvin) θ, the change in volume fraction field distribution φ, and the stress components distributions (N.m^{-2}) σ_{zz} respectively against the vertical distance for

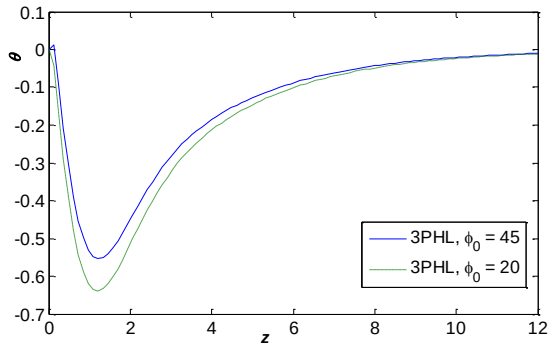

Fig. 11 Thermodynamics temperature θ for varying inclined load levels

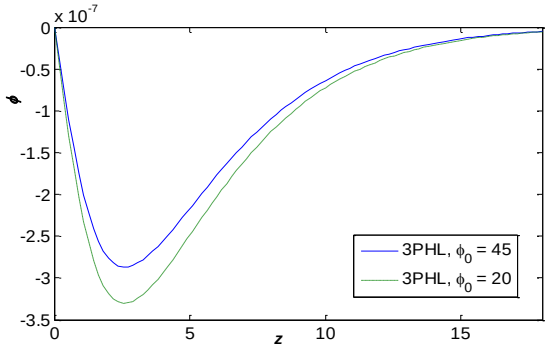

Fig. 12 The change in volume fraction field φ for varying inclined load levels

different values of the gravity field. Fig. 8 explains that variation of the thermodynamics temperature (θ) measures in Kelvin begins from a zero value that obeys the boundary conditions. The gravity field decreases values of θ. Fig. 9 depicts that the variation of change in the volume fraction field φ start from a zero value verified by the boundary condition. The gravity field decreases values of φ. Fig. 10 shows that the variation of the stress component σ_{zz} (N.m^{-2}) begins from a negative value and obeys the boundary condition. The gravity field increases values of σ_{zz}.

Figs. 11-13 represent the thermodynamic temperature distribution (Kelvin) θ, the change in volume fraction field distribution φ, and the stress components distributions (N.m^{-2}) σ_{zz} respectively against the vertical distance for different values of the inclined load. Fig. 11 explains that variation of the thermodynamics temperature (θ) measures in Kelvin begins from a zero value that obeys the boundary conditions. The inclined load increases values of θ. Fig. 12 depicts that the variation of change in the volume fraction field φ start from a zero value verified by the boundary condition. The inclined load increases values of φ. Fig. 13 shows that the variation of the stress component σ_{zz} (N.m^{-2}) begins from a negative value and obeys the boundary condition. The inclined load decreases values of σ_{zz}.

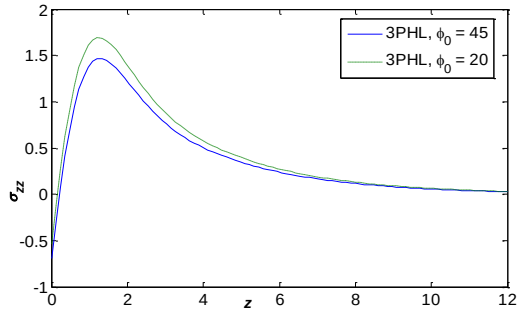

Fig. 13 Distribution of stress component σ_{zz} for varying inclined load levels

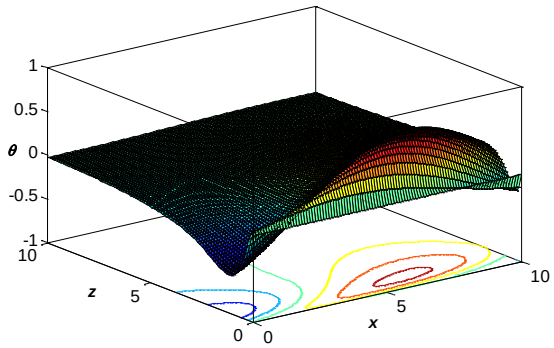

Fig. 14 Thermodynamics temperature θ in the context of 3PHL

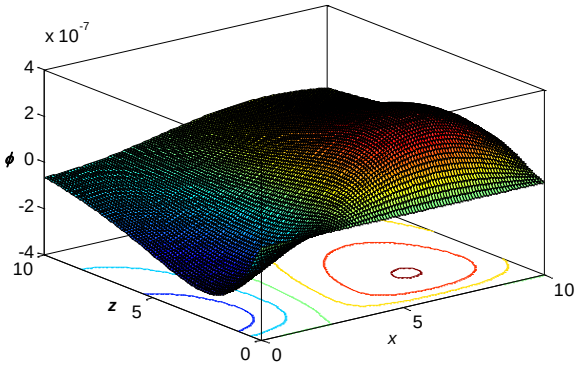

Fig. 15 Variation of change in volume fraction field φ in the context of 3PHL

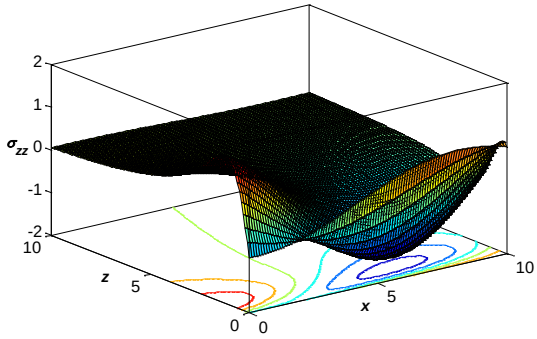

Fig. 16 Distribution of stress component σ_{zz} in the context of 3PHL

Finally, we added some 3D graphs (Figs. 14-16) to depict how the physical quantities change depending on the vertical distance. Interestingly, we observed from Fig. 14 that thermodynamic temperature varies θ with z for all values of x. But somewhere in x range, it is increasing and somewhere it is decreasing. Similar trends are found in Figs. 15 and 16 for the change in volume fraction field distribution φ, and the stress component σ_{zz}.

6. Conclusions

In the current work, wave propagations on a poro-thermoelastic half-space with temperature-dependent features and an inclined load are investigated within the framework of the 3PHL model using the normal mode analysis. The research mentioned above leads to the following conclusions:

- It is discovered that every field under consideration is sensitive to the gravity field.
- The thermoelastic problem in solids has analytical solutions that are based on normal mode analysis that have been created and applied.
- When examining the physical behavior of poro-thermoelastic materials, the magnetic field is crucial.
- The physical quantities under consideration are significantly affected by the inclined load, and all the examined fields are found to be sensitive to the empirical material constant.
- The physical quantities under inquiry are significantly impacted by the vertical distance.
- The method that was used in the present article is applicable to a wide range of problems in hydrodynamics and thermoelasticity.
- The three-phase-lag model is a mathematical model that includes the heat flux vector, the temperature gradient, and the thermal displacement gradient, which are useful in the problems of heat transfer, heat conduction, nuclear boiling, exothermic catalytic reactions, phonon-electron interactions, and phonon-scattering. So the 3PHL model is the most adequate theory to describe the present problem.

Acknowledgments

The authors thank Taif University Researchers Supporting Project Number (TURSP-2020/230), Taif University, Taif, Saudi Arabia.

Declaration of conflicting interests

The authors declared no potential conflicts of interest with respect to the research, authorship, and/or publication of this article.

Funding

This research received funding from "Taif University Researchers Supporting Project Number (TURSP-2020/230), Taif University, Taif, Saudi Arabia".

References

Abbas, I.A. (2015), "Generalized thermoelastic interaction in functional graded material with fractional order three-phase lag heat transfer", *J. Cent. South Univ.*, **22**, 1606-1613. https://doi.org/10.1007/s11771-015-2677-5.

Abbas, I., Hobiny, A. and Marin, M. (2020), "Photo-thermal interactions in a semi-conductor material with cylindrical cavities and variable thermal conductivity", *J. Taibah Univ. Sci*., **14**(1), 1369-1376. https://doi.org/10.1080/16583655.2020.1824465.

Abd-Alla, A.M., Abo-Dahab, S.M. and Hammed, H.A.H. (2011), "Propagation of Rayleigh waves in generalized magneto-thermoelastic orthotropic material under initial stress and gravity field", *Appl. Math. Model*., **35**(6), 2981-3000. https://doi.org/10.1016/j.apm.2010.11.067.

Abouelregal, A.E. and Zenkour, A. (2016), "Generalized thermoelastic interactions due to an inclined load at a two-temperature half-space", *J. Theor. Appl. Mech*., **54**(3), 827-838. https://doi.org/10.15632/jtam-pl.54.3.827.

Ahmed, S.M. (2005), "Stoneley waves in a non-homogeneous orthotropic granular medium under the influence of gravity", *Int. J. Math. Math. Sci*., **19**, 3145-3155. https://doi.org/10.1155/IJMMS.2005.3145.

Alharbi, A.M. (2021), "Two temperature theory on a micropolar thermoelastic media with voids under the effect of inclined load via three-phase-lag model", *ZAMM*, **101**(12), e202100078. https://doi.org/10.1002/zamm.202100078.

Alharbi, A.M., Said, S.M. and Othman, M.I.A. (2021), "Effect of gravity on a magneto-thermoelastic porous medium with the frame of a memory-dependent derivative in the context of the 3PHL model", *Steel Compos. Struct*., **40**(6), 881-891. https://doi.org/10.12989/scs.2021.40.6.881.

Alzahrani, F.S. and Abbas, I.A. (2019), "Analytical estimations of temperature in a living tissue generated by laser irradiation using experimental data", *J. Therm. Biol.*, **85**, 102421. https://doi.org/10.1016/j.jtherbio.2019.102421.

Biot, M.A. (1965), "Mechanics of Incremental Deformation", John Wiley & Sons, New York, NY, USA. https://hal.science/hal-01352219.

Biswas, S. (2021), "Rayleigh waves in porous orthotropic medium with phase lags", *Struct. Eng. Mech.*, **80** (3), 265-274. https://doi.org/10.12989/sem.2021.80.3.265.

Bromwich, T.J.J.A. (1898), "On the influence of gravity on elastic waves and in particular on the vibrations of an elastic globe", *Proc. Lon. Math. Soc*., **30** (1), 98-165. https://doi.org/10.1112/plms/s1-30.1.98.

Ciarletta, M. and Scalia, A. (1993), "On the nonlinear theory of nonsimple thermoelastic materials with voids", *ZAMM*, **73**(2), 67-75. https://doi.org/10.1002/zamm.19930730202.

Choudhuri, S.K.R. (2007), "On thermoelastic three phase lag model", *J. Therm. Stress*., **30**(3), 231-238. https://doi.org/10.1080/01495730601130919.

Cowin, S.C. and Nunziato, J.W. (1973), "Linear elastic materials with voids", *J. Elast*., **13**(7), 125-147. https://doi.org/10.1007/BF00041230.

De, A., Purkait, P., Das, P. and Kanoria, M. (2023), "Effect of magnetic field and inclined load on a two-dimensional thermoelastic medium under gravity", *J. Multi. Model*., **14**(3), 2350007. https://doi.org/10.1142/S1756973723500075.

Deswal, S., Poonia, R. and Kalkal, K.K. (2020), " Disturbances in an initially stressed fiber-reinforced orthotropic thermoelastic medium due to inclined load", *J. Braz. Soc. Mech. Sci. Eng*., **42**, 1-15. https://doi.org/10.1007/s40430-020-02338-x.

Fahmy, M.A. (2011), "A time-stepping drbem for magneto-thermo-viscoelastic interactions in a rotating nonhomogeneous anisotropic solid", *Int. J. Appl. Mech*., **3**(4), 711-734. https://doi.org/10.1142/S1758825111001202.

Fahmy, M.A. (2018)," Shape design sensitivity and optimization for two-temperature generalized magneto-thermoelastic problems using time-domain DRBEM", *J. Therm. Stress*., **41**(1), 119-138. https://doi.org/10.1080/01495739.2017.1387880.

Fahmy, M.A. (2019a),"Design optimization for a simulation of rotating anisotropic viscoelastic porous structures using time-domain OQBEM", *Math. Comp. Simul*., **166**, 193-205. https://doi.org/10.1016/j.matcom.2019.05.004.

Fahmy, M.A. (2019b), "A new boundary element strategy for modeling and simulation of three-temperature nonlinear generalized micropolar-magneto-thermoelastic wave propagation problems in FGA structures", *Eng. Anal. Bound. Elem*., **108**, 192-200. https://doi.org/10.1016/j.enganabound.2019.08.006.

Fahmy, M.A. (2019c),"A new convolution variational boundary element technique for design sensitivity analysis and topology optimization of anisotropic thermo-poroelastic structures", *Arab. J. Basic Appl. Sci*., **27**(1), 1-12. https://doi.org/10.1080/25765299.2019.1703493.

Fahmy, M.A. (2021a), "A new BEM for fractional nonlinear generalized porothermoelastic wave propagation problems", *Comp. Mater. Contin*., **68**(1), 59-76. https://doi.org/10.32604/Cmc.2021.015115.

Fahmy, M.A., Shaw, S., Mondal, S., Abouelregal, A.E., Lotfy, K.H., Kudinov, I.A. and Soliman, A.H. (2021b), "Boundary element modeling for simulation and optimization of three-temperature anisotropic micropolar magneto-thermoviscoelastic problems in porous smart structures using NURBS and genetic algorithm", *Int. J. Thermophys.*, **42**, 29. https://doi.org/10.1007/s10765-020-02777-7.

Fahmy, M.A., Alsulami, M.O. and Abouelregal, A.E. (2023), "Three-temperature boundary element modeling of ultrasound wave propagation in anisotropic viscoelastic porous media", *Axioms*, **12**(5), 473. https://doi.org/10.3390/axioms12050473.

Hetnarski, R.B. and Eslami, M.R. (2009), "Thermal stress-advanced theory and applications", (Springer Science Business Media, B.V., New York. https://link.springer.com/book/10.1007/978-1-4020-9247-3.

Hobiny, A.D. and Abbas, I.A. (2020), "Fractional order thermoelastic wave assessment in a two-dimension medium with voids", *Geomech. Eng.*, **21**(1), 85-93. https://doi.org/10.12989/gae.2020.21.1.085.

Hobiny, A. and Abbas, I. (2021a), "Analytical solutions of fractional bioheat model in a spherical tissue", *Mech. Based. Des. Struct. Mach.*, **49**(3), 430-439. https://doi.org/10.1080/15397734.2019.1702055.

Iesan, D. (1986), "A theory of thermoelastic material with voids", *Acta Mech*., **60**(6), 67-89. https://doi.org/10.1007/BF01302942.

Jain, K., Kalkal, K.K. and Deswal, S. (2018), "Effect of heat source and gravity on a fractional order fiber reinforced thermoelastic medium", *Struct. Eng. Mech*., **68**(2), 215-226. https://doi.org/10.12989/sem.2018.68.2.215.

Kumar, R. and Rani, L. (2006), "Deformation due to moving loads in thermoelastic body with voids", *Int. J. Appl. Mech. Eng.*, **11**(1), 37-59. http://content.sciendo.com/view/journals/ijame/ijame-overview.xml.

Kumar, R. and Aliwalia, P. (2007), "Interactions due to time harmonic inclined load in micropolar thermoelastic medium possesing cubic symmetry without energy dissipation", *Sci. Eng. Compos. Mater.* , **14**(3), 229-240. https://www.degruyter.com › SECM.2007.14.3.229.

Lata, P. and Singh, B. (2019a), "Effect of nonlocal parameter on nonlocal thermoelastic solid due to inclined load", *Steel Compos. Struct*., **33**(1), 123-131. https://doi.org/10.12989/scs.2019.33.1.123.

Lata P. and Kaur, I. (2019b), "Effect of rotation and inclined load on transversely isotropic magneto thermoelastic solid", *Struct. Eng. Mech.*, **70** (2), 245-255. https://doi.org/10.12989/sem.2019.70.2.245.

Lata, P. and Himanshi, H. (2022), "Inclined load effect in an orthotropic magneto-thermoelastic solid with fractional order heat transfer", *Struct. Eng. Mech*., **81**(5), 529-537. https://doi.org/10.12989/sem.2022.81.5.529.

Marin, M. (1996), "Some basic theorems in elastostatics of micropolar materials with voids", *J. Comput. Appl. Math*., **70**(1), 115-126. https://doi.org/10.1016/0377-0427(95)00137-9.

Marin, M. (1997), "On the domain of influence in thermoelasticity of bodies with voids", *Arch. Math.* (Brno)., **33**(4), 301-308. http://dml.cz/dmlcz/107618.

Marin, M., Othman, M.I.A. and Abbas, I.A. (2015), "An extension of the domain of influence theorem for anisotropic thermoelastic material with voids", *J. Comput. Theor. Nanosci*., **12**(8), 1594-1598.

Marin, M., Hobiny, A. and Abbas, I. (2021b), "The effects of fractional time derivatives in porothermoelastic materials using finite element method", *Math.*, **9**(14), 1606. https://doi.org/10.3390/math9141606.

Marin, M., Seadawy, A., Vlase, S. and Chirila, A. (2022), "On mixed problem in thermos-elasticity of type III for Cosserat media", *J. Taibah Univ. Sci*., **16**(1), 1264-1274. https://doi.org/10.1080/16583655.2022.21602.

Nath, S. and Sengupta, P.R. (1999), "Influence of gravity on propagation of waves in a medium in presence of a compressional source", *Sadhana*, **24**(12), 495-505. https://doi.org/10.1007/BF02745625.

Nunziato, J.W. and Cowin, S.C. (1979), "A nonlinear theory of elastic materials with voids", *Arch. Rat. Mech. Anal*., **72**(6), 175-201. https://doi.org/10.1007/BF00249363.

Othman, M.I.A., Lotfy, K.H. and Farouk, R.M. (2009), "Effects of magnetic field and inclined load in micropolar thermoelastic medium possessing cubic symmetry under three theories", *Int. J. Ind. Math.*, **1**(2), 87-104. http://ijim.srbiau.ac.ir.

Othman, M.I.A., Elmaklizi, Y.D. and Said, S.M. (2013), "Generalized thermoelastic medium with temperature dependent properties for different theories under the effect of gravity field", *Int. J. Thermophys*., **34**(3), 521-537. https://doi.org/10.1007/s10765-013-1425-z.

Othman, M.I.A., Fekry, M. and Marin, M. (2020), "Plane waves in generalized magneto-thermo-viscoelastic medium with voids under the effect of initial stress and laser pulse heating", *Struct. Eng. Mech*., **73** (6), 621-629. https://doi.org/10.12989/sem.2020.73.6.621.

Quintanilla, R (2009), "Uniqueness in thermoelasticity of porous media with micro-temperatures", *Arch. Mech.*, **61**(5), 371-382. https://am.ippt.pan.pl/am/article/viewFile/v61p371/pdf.

Said, S.M., Othman, M.I.A. and Eldemerdash, M.G. (2022), "A novel model on nonlocal thermoelastic rotating porous medium with memory-dependent derivative", *Multi. Model. Mater. Struct*., **18**(5), 793-807. https://doi.org/10.1108/MMMS-05-2022-0085.

Said, S.M., Abd–Elaziz, E.M. and Othman, M.I.A. (2023), "A modified couple-stress magneto–thermoelastic solid with microtemperatures and gravity field", *Struct. Eng. Mech*., **87**(5), 475-485. https://doi.org/10.12989/sem.2023.87.5.475.

Said, S.M. (2024), "Effect of the gravity on a nonlocal micropolar thermoelastic media with the multi-phase-lag model", *Geomech. Eng.*, **36**(1), 19-26. https://doi.org/10.12989/gae.2024.36.1.019.

. Sharma, N., Kumar, R. and Lata, P. (2015), "Disturbance due to inclined load in transversely isotropic thermoelastic medium with two temperatures and without energy dissipation", *Mater. Phys. Mech*., **22**(2), 107-117. https://api.semanticscholar.org/CorpusID:201928700.

Tantawy, R.M. and Zenkour, A.M. (2023), "Effects of porosity, rotation, thermomagnetic, and thickness variation on functionally graded tapered annular disks", *Inf. Sci. Lett*., **12**(3), 1133-1150. https://doi.org/10.18576/isl/120305.

Zenkour, A.M. (2020), "Wave propagation of a gravitated piezo-thermoelastic half-space via a refined multi-phase-lags theory", *Mech. Adv. Mater. Struct*., **27**(22), 1923-1934. https://doi.org/10.1080/15376494.2018.1533057.

JS

Appendix

$$\pi = 1 + \frac{\varepsilon_0 \mu_0^2 H_0^2}{\rho}, \qquad \pi_0 = \frac{\gamma \alpha_3 T_0}{\rho C_E (\lambda + 2\mu)}, \qquad \pi_1 = \frac{\mu}{\rho c_1^2}, \quad \pi_2 = \frac{\lambda + \mu}{\rho c_1^2},$$

$$\pi_5 = 1 + \pi_4 H_0, \quad \pi_6 = \pi_2 + \pi_4 H_0,$$

$$\pi_3 = \frac{b}{\rho c_1^2}, \quad \pi_4 = \frac{\mu_0 H_0^2}{\rho c_1^2},$$

$$\pi_7 = \frac{\gamma^2 T_0}{\rho C_E (\lambda + 2\mu)}, \qquad \pi_8 = \frac{\eta K}{\rho C_E}, \qquad \pi_9 = \frac{K^*}{\rho C_E c_1^2}, \qquad \varpi_1 = \frac{b}{\beta c_1^2 \eta^2},$$

$$\varpi_2 = \frac{\alpha_1}{\beta c_1^2 \eta^2}, \qquad \varpi_3 = \frac{\alpha_2}{\beta \eta}, \qquad \varpi_4 = \frac{\alpha_3 (\lambda + 2\mu)}{\gamma \beta c_1^2 \eta^2}, \qquad \pi_5 = \frac{\rho \alpha_4 c_1^2}{\beta} .$$

$$\pi_{10} = \pi_5 B^2 + \pi m^2, \qquad \pi_{11} = \pi_1 B^2 + \pi m^2, \qquad \pi_{12} = B^2 + \varpi_2 + \varpi_3 m + \varpi_5 m^2,$$

$$\pi_{13} = m_2 + m_3, \quad \pi_{14} = \pi_{13} B^2 + m_1, \qquad m_1 = m^2 \left(1 + m\tau_q + 0.5 m^2 \tau_q^2\right),$$

$$m_2 = m\pi_8 \left(1 + m\tau_T\right), \qquad m_3 = \pi_9 \left(1 + m\tau_\upsilon\right), \qquad \mathrm{D} = \frac{d}{dz} ,$$

$$\chi_1 = \frac{1}{\pi_1 \pi_5 \pi_{13}} \left(\pi_{13}\pi_{15} + \pi_1 \pi_{16}\right),$$

$$\chi_2 = \frac{1}{\pi_1 \pi_5 \pi_{13}} \left(\pi_{10}\pi_{16} + \pi_7 \pi_{17} m_1 + B^2 \pi_{13}\pi_{19} - \pi_{14}\pi_{18} + \pi_{13}\pi_{20} + \pi_1 \pi_{24}\right)$$

$$\chi_3 = \frac{1}{\pi_1 \pi_5 \pi_{13}} \left(m_1 \pi_7 \pi_{21} + B^2 \pi_{14}\pi_{19} + \pi_{10}\pi_{14}\pi_{22} - B^2 g^2 \pi_{12}\pi_{13} + \pi_{11}\pi_{23} + m_1 \pi_0 \pi_{25}\right)$$

$$\chi_4 = \frac{1}{\pi_1 \pi_5 \pi_{13}} \left(B^2 m_1 \pi_{11}\pi_7 \pi_{12} - B^2 \varpi_4 \pi_3 \pi_7 \pi_{11} m_1 - B^2 \varpi_1 \pi_3 \pi_{14} \pi_{11} + \pi_{10}\pi_{11}\pi_{12}\pi_{14} - B^2 g^2 \pi_{12}\pi_{14} + \pi_{26}\right)$$

$$\pi_{15} = \pi_1 \pi_{11} + \pi_5 \pi_{10} + \pi_1 \pi_5 \pi_{12} - B^2 \pi_6^2, \qquad \pi_{16} = \pi_5 \pi_{14} - b\pi_3 \pi_{13} + \pi_7 m_1,$$

$$\pi_{17} = \pi_1 \pi_{12} - 2B^2 \pi_6 + B^2 \pi_5 - \pi_1 \pi_3 \varpi_4,$$

$$\pi_{18} = -\pi_1 \pi_{11} + \pi_1 \pi_3 \varpi_1 + B^2 \pi_6^2 - \pi_1 \pi_{12} \pi_5,$$

$$\pi_{19} = 2\pi_3 \pi_6 \varpi_1 - \pi_3 \pi_5 \varpi_1 - \pi_6^2 \pi_{12} - g^2, \qquad \pi_{20} = \pi_0 \pi_{11} + \pi_1 \pi_{11} \pi_{12} + \pi_5 \pi_{10} \pi_{12},$$

$$\pi_{21} = B^2 \pi_{11} - 2B^2 \pi_6 \pi_{12} + 2\varpi_4 \pi_3 \pi_6 B^2 + B^2 \pi_5 \pi_{12} - B^2 \pi_3 \pi_5 \varpi_4 + \pi_{10}\pi_{12} - \pi_3 \pi_{10} \varpi_4,$$

$$\pi_{22} = \pi_{11} + \pi_5 \pi_{12} - \pi_3 \varpi_1,$$

$$\pi_{23} = -B^2 \varpi_1 \pi_3 \pi_{13} + \pi_{13}\pi_{10}\pi_{12} + \pi_1 \pi_{12} \pi_{14} + \varpi_4 \pi_0 \pi_1 m_1,$$

$$\pi_{24} = \varpi_4 \pi_0 \pi_5 m_1 - \varpi_1 \pi_0 m_1,$$

$$\pi_{25} = 2B^2 \pi_6 \varpi_1 - B^2 \varpi_1 \pi_5 + \pi_5 \pi_{10} \varpi_4 - \varpi_1 \pi_{10} - \pi_6^2 B^2 \varpi_4,$$

$$\pi_{26} = -m_1 B^2 \varpi_1 \pi_0 \pi_{11} + \pi_{11}\pi_0 \pi_{10} m_1 \varpi_4 - B^2 g^2 \pi_0 m_1 \varpi_4.$$

$$\Delta_{1n} = \frac{A_{1n}}{B_{1n}}, \quad \Delta_{2n} = \frac{A_{2n}}{B_{2n}}, \quad \Delta_{3n} = \frac{A_{3n}}{B_{3n}},$$

$$A_{1n} = \pi_1 R_n^3 + (B^2 \pi_6 - \pi_{10}) R_n + B^2 g \qquad ,$$

$$B_{1n} = \mathrm{i}\, B (\pi_6 R_n^2 - \pi_5 R_n^2 - g R_n + \pi_{11}),$$

$$B_{2n} = \mathrm{i}\, B (m_1 \pi_0 - \pi_3 \pi_{13} R_n^2 + \pi_3 \pi_{14}) \quad , \quad A_{3n} = \varpi_4 \Gamma_{2n} - \mathrm{i} B \varpi_1 + \varpi_1 R_n \Gamma_{1n} \quad ,$$

$$B_{3n} = \pi_{12} - R_n^2,$$

List of Symbols

σ_{ij}	components of stress tensor
e_{ij}	components of strain tensor
T	absolute temperature
T_0	temperature of medium in its natural state assumed to be such that $\left\|(\mathrm{T} - T_0)/T_0\right\| < 1$, $\theta_0 = T - T_0$
τ_T	the phase-lag of temperature gradient
τ_q	the phase-lag of heat flux
τ_v	the phase-lag of thermal displacement gradient
$\mu_1, \lambda_1, \gamma_1$	constants of material
$\beta, b, \alpha_1, \alpha_2,$ α_3, α_4	the material constants due to the presence of voids
u_i	the displacement components
λ, μ	Lame's constant
δ_{ij}	Kronecker's delta
K^*	coefficient of thermal conductivity
K	the additional material constant
ρ	density
C_E	specific heat at constant strain
θ_0	an empirical material constant
i	imaginary unit, $\mathrm{i} = \sqrt{-1}$
B	wave number
m	complex constant
α_t	linear thermal expansion coefficient, $\gamma = (3\lambda + 2\mu)\alpha_t$,
φ	the change in volume fraction field of voids
μ_0	the magnetic permeability
ε_0	the electric permeability
$\mu_0 (\boldsymbol{J} \times \boldsymbol{H})_i$	the Lorentz force